Registration of MR Images to Ultrasound Images of the Spine

Lars Eirik Bø[1,2,3], Rafael Palomar[4], Tormod Selbekk[1], and Ingerid Reinertsen[1,2]

[1]SINTEF Technology and Society, Trondheim, Norway
[2]Norwegian University of Science and Technology, Trondheim, Norway
[3]The Central Norway Regional Health Authority, Trondheim, Norway
[4]The Intervention Centre, Oslo University Hospital, Oslo, Norway

May 19, 2014

Abstract

One of the main limitations of today's navigation systems for spine surgery is that they often are not available until after the bone surface has been exposed. Also, they lack the capability of soft tissue imaging, both preoperatively and intraoperatively. The use of ultrasound has been proposed to overcome these limitations. By registering preoperative magnetic resonance (MR) images to intraoperative percutaneous ultrasound images, navigation can start even before incision. We therefore present a method for registration of MR images to ultrasound images of the spine. The method is feature-based and consists of two steps: segmentation of the bone surfaces from both the ultrasound images and the MR images, followed by rigid registration using a modified version of the Iterative Closest Point algorithm. The method was tested on data from a healthy volunteer, and the data set was successfully segmented and registered with an accuracy of 3.67 ± 0.38 mm.

1 Introduction

In spinal surgery today, many procedures are performed with no or only minimal image guidance. Preoperative computed tomography (CT) or magnetic resonance (MR) images are used for diagnosis and planning, but during surgery, two-dimensional C-arm fluoroscopy is widely used both for initial

*Originally published in J. Yao, T. Klinder and S. Li (eds.) 2014, *Computational Methods and Clinical Applications for Spine Imaging*, Springer, pp. 209–218

detection of the correct spinal level and for intra-operative imaging. Navigation systems exist, but mainly for placement of pedicle screws. These usually first come to use when the bone surface has been exposed. Using a simple landmark or surface registration method the preoperative CT image is then aligned with the patient and can be used for planning and guidance of the screws. A number of groups have evaluated the use of navigation for this purpose, and a review of the topic was presented by Tjardes et al. [12]. They conclude that the benefits of image-guidance in terms of accurate placement of the screws and reduced exposure to ionizing radiation have been proven, in particular for the cervical and lumbar procedures. In other areas of spine surgery, navigation and image guidance are still on the experimental stage.

One of the main limitations of today's navigation systems for spine surgery is that they often are not available until after the bone surface has been exposed. The use of ultrasound has been proposed to overcome this limitation. By registering preoperative images to intraoperative percutaneous ultrasound images, navigation can start before incision and therefore be used for both level detection and planning at an early stage of the procedure. Thus, the use of X-ray fluoroscopy can possibly be reduced.

In order to make a navigation system based on intraoperative ultrasound clinically useful, the greatest challenge is to achieve accurate and robust registration between the preoperative images and the ultrasound images with minimal user interaction. Registration of CT images of the spine to corresponding ultrasound images has been investigated by several groups, and two main approaches have been explored: feature-based registration and intensity-based registration. In the first case, corresponding features are extracted from the two datasets to be registered prior to registration. In the case of spine surgery, the feature of choice is the bone surface as this is the only feature that can be reliably detected in the ultrasound images. Segmentation of the bone surface from ultrasound images of the spine is still a challenging topic due to noise, artifacts and difficulties in imaging surfaces parallel to the ultrasound beam. A few methods have been described in the literature, ranging from simple ray tracing techniques [15] to more advanced methods based on probability measures [7, 4, 9] or phase symmetry [13]. Following surface extraction, the segmented bone surfaces are registered using the Iterative Closest Point (ICP) algorithm [2] or the unscented Kalman filter [9].

In intensity-based registration, a similarity metric based on the image intensities is optimized to find the spatial transformation that best maps one image onto the other [14, 8, 6, 15]. As MR/CT and ultrasound images present very different intensity and noise characteristics, a common approach is to create simulated ultrasound images from the pre-operative data and register the simulated image to the real ultrasound image. In these simulations, the direction of sound wave propagation, transmission, reflection

and noise can be modelled in order to obtain images that can be reliably registered to real ultrasound images based on image intensities.

While these studies show a lot of promise, they focus almost exclusively on the registration of preoperative CT images. However, many spinal procedures, such as the treatment of disc herniations and intraspinal tumours, rely on the soft-tissue imaging capabilities of MR. Thus, by combining ultrasound imaging with preoperative MR, navigation could be extended to a variety of spinal procedures that do not benefit from image guidance today. In these procedures, the ultrasound could also be used for intraoperative imaging, reducing the use of fluoroscopy even further. As a first step towards this end, we present a method for registration of preoperative MR images to percutaneous ultrasound images of the spine, including a preliminary assessment of its performance.

2 Methods and Experiments

Our registration method is feature-based and consists of two steps: First, the bone surfaces are segmented from both the ultrasound images and the MR images, and then the two surfaces are registered using a modified version of the ICP algorithm.

2.1 Ultrasound Acquisition and Segmentation

The ultrasound images were acquired using a Vivid E9 scanner with an 11 MHz linear probe (GE Healthcare, Little Chalfont, UK). Some groups have used lower frequencies, which enable good imaging of deeper structures such as the transverse processes of the spine [15, 9, 13, 14, 6]. However, this makes imaging of superficial structures, such as the spinous processes and the sacrum, challenging. As these structures represent important features for the registration algorithm, we found that a relatively high frequency gave a better compromise between depth penetration and resolution. The ultrasound probe was tracked with the Polaris optical tracking system (NDI, Waterloo, ON, Canada), and both images and corresponding tracking data were recorded using the navigation system CustusX [1] with a digital interface to both the ultrasound scanner and the tracking system. The two-dimensional ultrasound images were also reconstructed to a three-dimensional volume using the Pixel Nearest Neighbor (PNN) reconstruction algorithm [11].

While the reconstructed, three-dimensional ultrasound volume is useful for navigation, the reconstruction process tends to introduce a certain blurring. The volume usually also has a lower resolution than the original, two-dimensional ultrasound images. We therefore used the latter as input to our segmentation method. In order to extract the bone surfaces from these images, we used a combination of the bone probability maps introduced by Jain et al. [7] and Foroughi et al. [4], and the backward scan line tracing

presented by Yan et al. [15]. In ultrasound images, reflections from bone surfaces are seen as bright ridges perpendicular to the ultrasound beam. To calculate the probability of each pixel $a^{i,j}$ of the image A being part of such a ridge, the image was smoothed with a Gaussian filter, before calculating the Laplacian of Gaussian (LoG), i.e.

$$A_{\mathrm{G}} = \{a_{\mathrm{G}}^{i,j}\} = A * G \qquad \text{and} \qquad A_{\mathrm{LoG}} = \{a_{\mathrm{LoG}}^{i,j}\} = A_{\mathrm{G}} * L \ , \tag{1}$$

where G and L are the convolution kernels of the Gaussian filter and the LoG filter respectively. This is a common operation in blob detection and usually produces a strong positive response for dark blobs and a strong negative response for bright blobs. To enhance the bright reflections, the positive values were therefore set to zero before taking the absolute value of the rest. The result was then added to the smoothed version of the original image to produce an initial bone probability map $P_1 = \{p_1^{i,j}\}$, i.e.

$$p_1^{i,j} = a_{\mathrm{G}}^{i,j} + |\max\{a_{\mathrm{LoG}}^{i,j}, 0\}| \ . \tag{2}$$

The other feature to be considered was the intensity profile in the propagation direction of the ultrasound. For a bone surface, this is typically characterized by a sudden, sharp peak followed by a dark shadow. To calculate the probability of a given pixel representing the maximum of such a profile, each scan line was considered separately. Assuming p_1^m is the mth pixel of the initial bone probability map P_1 along a given scan line, the secondary bone probability of this pixel was found as

$$p_2^m = p_1^m - \frac{p_1^{m-\delta} + p_1^{m+\delta}}{2} - \frac{\omega}{\lambda} \sum_{n=1}^{\lambda} p_1^{m+\delta+n} \ , \tag{3}$$

where 2δ is the width of a typical intensity peak and λ is the length of a typical bone shadow, both given in pixels. In our case, these were set to $\delta = 24$ and $\lambda = 322$, which corresponds to 1.5 mm and 20 mm respectively. ω is a weight that can be adjusted according to the overall noise level of the bone shadows in the image, and in our case this was set to 10.

The first term in (3) is simply the intensity of the mth pixel. At a bone reflection, this will be high and lead to a high bone probability. The second term combines the intensities at the distance δ behind and in front of the mth pixel. At a sharp peak of width 2δ, both of these will be low and have little impact on the bone probability. On the other hand, if there is no such peak, at least one of these will be high and lead to a reduced bone probability. The last term is the average intensity of the pixels in the shadow region behind the peak. If there is a lot of signal in this area, this term will be high and thus reducing the bone probability

Finally, we applied a variant of the backward scan line tracing to the resulting probability map: For each scan line, starting at the bottom of the

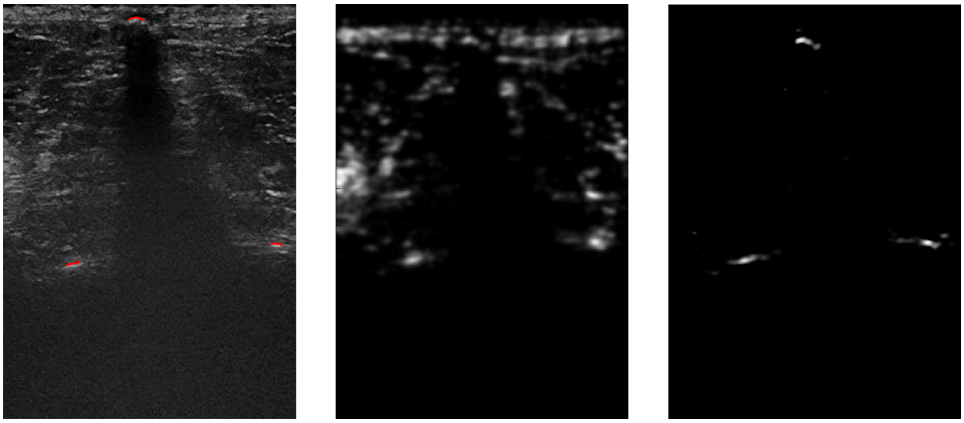

Figure 1: An ultrasound image of a vertebra with the segmentation overlaid in red (left), the initial bone probability map (centre) and the final bone probability map after applying the threshold (right).

image, the first local maximum above a certain threshold was deemed part of a bone surface. This was repeated for all the recorded images, and based on the corresponding tracking data, all points were transformed into the three-dimensional reference space of the tracking system. A typical example of both the probability maps and the final segmentation of an image is shown in Fig. 1. The method was implemented in MATLAB (MathWorks, Natick, MA, USA).

2.2 MR Acquisition and Segmentation

The MR images were acquired using an Achieva 3.0 T scanner (Philips Healthcare, Amsterdam, Netherlands). In order to facilitate both the segmentation of the spine and the subsequent navigation, we customized a full, three-dimensional MR protocol which enhanced the contrast between the bone and the surrounding soft tissue. This had a field of view of $80 \times 560 \times 560$ voxels and a voxel size of $1 \times 0.48 \times 0.48\,\mathrm{mm}^3$. The lumbar vertebrae were segmented using a semiautomatic method based on active contours implemented in the segmentation software ITK-SNAP [16]. However, in the area of the sacrum, the contrast between the bone and the surrounding soft tissue was lower, and here active contours driven by robust statistics resulted in more accurate segmentations. For this part, we therefore employed the Robust Statistics Segmentation (RSS) module [5] included in the medical imaging analysis and visualization software 3D Slicer [3].

The use of active contours for segmentation may lead to oversegmentation of certain anatomical structures, known as leaks. In MR images, such leaks are especially prominent in areas with motion artifacts caused by the

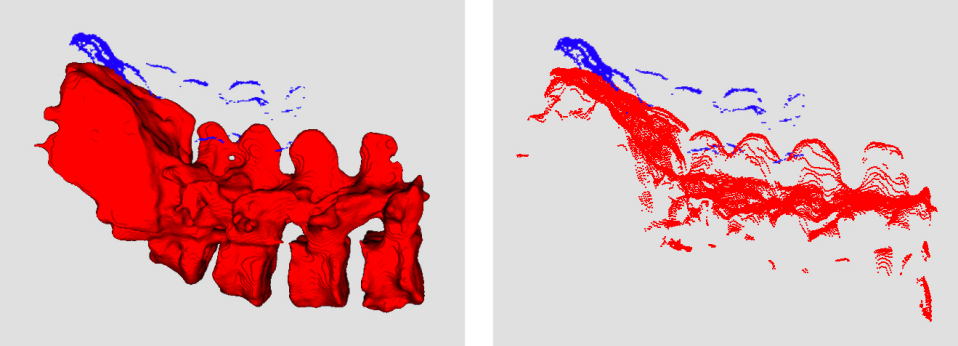

Figure 2: The segmented ultrasound (blue) and MR (red) surfaces (left) and the same surfaces after reducing the MR surface with ray tracing (right).

patient not lying completely still during the image acquisition. This is often a problem, especially for patients in need of spine surgery. To compensate for this, minor corrections of the segmentation results were performed manually for both the lumbar area and the sacrum.

The surface segmented from the MR volume represented the entire lumbar spine, and consisted therefore of a large number of points. However, only the surfaces facing the ultrasound probe were visible in the ultrasound images. Thus, a significant portion of the surface points in the segmented MR were irrelevant to the registration, as there were no corresponding points in the ultrasound images. To reduce the amount of data, and thus the work load of the registration algorithm, we therefore used a simple ray tracing method (posterior to anterior) to extract those points that were facing the ultrasound probe. An example of the resulting reduced surface can be seen in Fig. 2.

2.3 Registration

Following segmentation, the segmented surfaces from ultrasound and MR were imported into the navigation system for registration. Like all automatic registration methods, the ICP algorithm requires an initialization or a reasonable starting point in order to converge to the correct solution. This was provided by assuming that the two volumes covered approximately the same volume, that the first recorded ultrasound image was positioned at the sacrum and that the probe trajectory was from the sacrum upwards. The two image volumes were then aligned by first rotating the MR volume in order to align the x, y and z axes in the two volumes, and then translating the MR volume in order to align the points corresponding to the voxels $(n_x/2, 0, 0)$ in both volumes, where n_x is the number of voxels in the x-direction (patient left-to-right).

After this initial alignment, we used the ICP algorithm to rigidly regis-

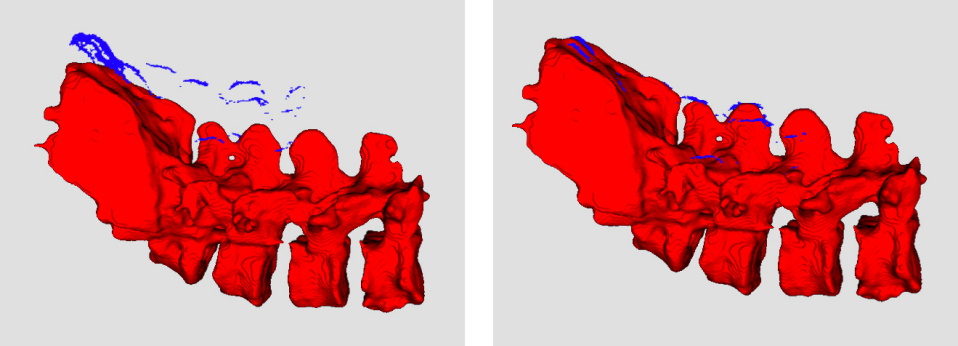

Figure 3: The ultrasound (blue) and MR (red) surfaces after the initial alignment (left) and after the final registration (right).

ter the reduced MR surface to the ultrasound surface. In order to reduce the influence of possible outliers on the registration result, the algorithm was modified by incorporating the Least Trimmed Squares (LTS) robust estimator as described by Reinertsen et al. [10].

2.4 Experiments

In order to evaluate our method, we acquired both ultrasound and MR images of the spine of a healthy volunteer. The only structures that were clearly discernible in both of these images were the top points of the spinous processes of three lowest vertebrae (L3, L4 and L5). These were therefore selected as control points and manually identified in both the original ultrasound volume and the MR volume. The surfaces were then registered to each other using the method described above, and the distances between the landmarks both after initial alignment and after final registration were computed.

3 Results

Through careful optimization of the acquisition protocols, both MR and ultrasound images of high quality were achieved. The data sets were successfully segmented and registered using the methods described above. Figure 3 shows the extracted surfaces both after the initial alignment and after rigid registration. The match can also be seen in Fig. 4, which shows transverse and sagittal views of corresponding ultrasound and MR volumes after registration. Finally, the distances between the control points before and after registration are given in Table 1.

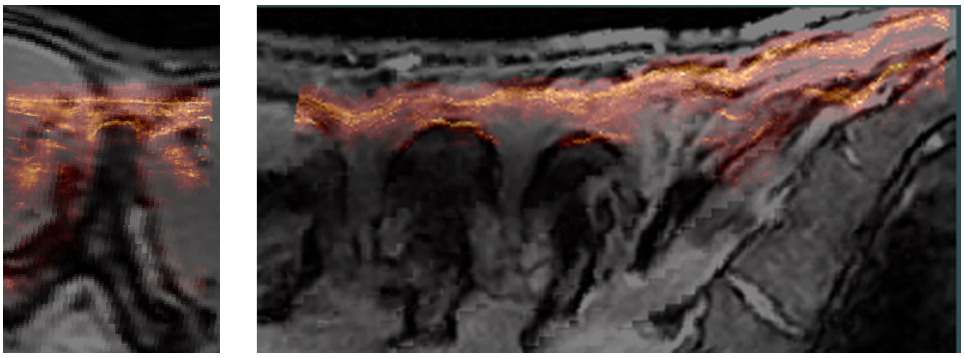

Figure 4: A transverse slice (left) and a sagittal slice (right) from the ultrasound volume overlaid on top of the corresponding slices from the registered MR volume. The ultrasound data is shown in red and yellow and the MR data is shown in grey tones.

Table 1: Distance between the control points in mm.

	L3	L4	L5	Mean±STD
After initial alignment	23.29	21.27	22.40	22.32±1.01
After final registration	3.86	3.93	3.23	3.67±0.38

4 Discussion

We have demonstrated that registration between MR and ultrasound images is feasible. The accuracy of 3.67 ± 0.38 mm is clinically relevant as it is sufficient to ensure that we are on the correct level. It is also comparable to that of many of the studies mentioned in the introduction. Still, this is a work in progress, and the results shown here are only preliminary.

It has been pointed out that intensity-based registration has an advantage over feature-based methods in that it makes use of all the information in the image, rather than just that of the bone surfaces [6]. In the case of spine imaging, however, other structures that are visible in the ultrasound images, such as muscle fibres and fat layers, are not imaged very well by neither CT nor MR. Their contribution to the registration procedure is therefore questionable.

The ultrasound images that we have acquired vary considerably in appearance from subject to subject. At the moment, this means that the parameters of the segmentation method, such as the width δ of the reflections, the length λ of the shadows and the weight ω must be manually adjusted to the particular data set. In the future, these adjustment should be done automatically, e.g. based on overall image statistics.

The MR segmentation methods that we presented here are only semi-automatic and quite time consuming. However, the result of this was a complete segmentation of the lumbar spine, and as we have already pointed out, only a small part of this information was actually relevant to the registration. We are therefore investigating methods to segment only the part of the anatomy that is most critical to the registration, i.e. the sacrum and the spinous and transverse processes. The results are promising, and it should be possible to perform this segmentation both quickly and with minimal user interaction.

The last component of the method is the registration. Here, we have shown that a reasonable rigid registration can be achieved using the ICP algorithm. However, the spine is flexible, and the change in curvature from the MR scanner, where the patient is lying in a supine position, to the operating room, where the patient is placed in a prone position, can be large. A group-wise rigid registration method, like the one proposed e.g. by Gill et al. [6] where only the space between the vertebrae is deformed, would be more appropriate.

Finally, our method needs more extensive testing, both with respect to robustness to anatomical variations and with respect to accuracy. The distance measure that we have used here, based on manual identification of landmarks, gives a good indication of the registration accuracy, but we should include a measure of inter- and intra-observer variability. Such measures could therefore be complimented with other assessment methods, such as phantom studies where the exact geometry is known and a reliable ground

truth thus can be established. All of the above are currently addressed in our research.

5 Conclusion

The presented method is capable of registering MR images to percutaneous ultrasound images of the spine. The registration accuracy is clinically relevant, and with minor improvements the user interaction can be reduced to a minimum. This method is thus an important step towards the realisation of a system for MR- and ultrasound-guided spine surgery.

Acknowledgements

The work was funded through the user-driven research-based innovation project VIRTUS (The Research Council of Norway grant no. 219326, SonoWand AS) and through a PhD grant from the Liaison Committee between the Central Norway Regional Health Authority (RHA) and the Norwegian University of Science and Technology.

References

[1] C. Askeland et al. CustusX: A Research Application for Image-Guided Therapy. *The MIDAS Journal*, page 1–8, 2011.

[2] P. J. Besl et al. A Method for Registration of 3-D Shapes. *IEEE Transactions on Pattern Analysis and Machine Intelligence*, 14(2):239–256, 1992.

[3] A. Fedorov et al. 3D Slicer as an image computing platform for the Quantitative Imaging Network. *Magn Reson Imaging*, 30(9):1323–1341, 2012.

[4] P. Foroughi et al. Ultrasound Bone Segmentation Using Dynamic Programming. In M. P. Yuhas, editor, *2007 IEEE Ultrasonics Symposium*, page 2523–2526. IEEE, 2007.

[5] Y. Gao et al. A 3D interactive multi-object segmentation tool using local robust statistics driven active contours. *Med Image Anal*, 16(6): 1216–1227, 2012.

[6] S. Gill et al. Biomechanically constrained groupwise ultrasound to CT registration of the lumbar spine. *Med Image Anal*, 16(3):662–674, 2012.

[7] A. K. Jain et al. Understanding Bone responses in B-mode Ultrasound Images and Automatic Bone Surface extraction using a Bayesian Probabilistic Framework. In W. F. Walker and S. Y. Emelianov, editors, *Medical Imaging 2004: Ultrasonic Imaging and Signal Processing*, volume 5373 of *Proceedings of SPIE*, page 131–142. SPIE, 2004.

[8] A. Lang et al. Multi-modal registration of speckle-tracked freehand 3D ultrasound to CT in the lumbar spine. *Med Image Anal*, 16(3):675–686, 2012.

[9] A. Rasoulian et al. Feature-based multibody rigid registration of CT and ultrasound images of lumbar spine. *Med Phys*, 39(6):3154–3166, 2012.

[10] I. Reinertsen et al. Validation of vessel-based registration for correction of brain shift. *Med Image Anal*, 11(4):374–388, 2007.

[11] O. V. Solberg et al. 3D ultrasound reconstruction algorithms from analog and digital data. *Ultrasonics*, 51(4):405–419, 2011.

[12] T. Tjardes et al. Image-guided spine surgery: state of the art and future directions. *Eur Spine J*, 19(1):25–45, 2010.

[13] D. Tran et al. Automatic Detection of Lumbar Anatomy in Ultrasound Images of Human Subjects . *IEEE Trans Biomed Eng*, 57(9):2248–2256, 2010.

[14] S. Winter et al. Registration of CT and Intraoperative 3-D Ultrasound Images of the Spine Using Evolutionary and Gradient-Based Methods. *IEEE Transactions on Evolutionary Computation*, 12(3):284–296, 2008.

[15] C. X. B. Yan et al. Ultrasound-CT registration of vertebrae without reconstruction. *Int J Comput Assist Radiol Surg*, 7(6):901–909, 2012.

[16] P. A. Yushkevich et al. User-guided 3D active contour segmentation of anatomical structures: significantly improved efficiency and reliability. *NeuroImage*, 31(3):1116–1128, 2006.